EUROPEAN JOURNAL OF MATERIALS SCIENCE AND ENGINEERING
Volume 11, Issue 03, 2026: 179-204 | www.ejmse.ro | ISSN: 2537-4338

EJMSE

DOI: 10.36868/ejmse.2026.11.03.179

LONG-TERM EIS EVALUATION OF PCC-BASED Zn, Zr AND Ca ON Ti6Al4V IN DPBS

Diana-Petronela BURDUHOS-NERGIS[1][0000-0002-0680-9885], Andrei Victor SANDU[1,2][0000-0002-9292-749X], Luminita-Gabriela MUTILA, Costica BEJINARIU[1,2*][0000-0003-1973-7240] and Petrica VIZUREANU[1,2,3][0000-0002-3593-9400]

[1]"Gheorghe Asachi" Technical University of Iasi, Faculty of Materials Science and Engineering, 41 "D. Mangeron" Street, 700050, Iasi, Romania
[2]Academy of Romanian Scientists, 54 Splaiul Independentei St., Sect. 5, 050094 Bucharest, Romania;
[3]Technical Sciences Academy of Romania, 26 Dacia Blvd., 030167 Bucharest, Romania

Abstract

This study analysed the long-term evolution of the electrochemical behaviour of three phosphate conversion coatings (PCC) based on Zn, Zr and Ca, deposited on the titanium alloy Ti6Al4V. They were immersed for 30, 60 and 90 days in Dulbecco's Buffered Saline Solution (DPBS), with the electrochemical response being evaluated using electrochemical impedance spectroscopy (EIS). The Nyquist and Bode diagrams were interpreted, and modelling using equivalent electrical circuits was carried out, in order to highlight the differences between the three compositions and how they evolve over time. It was therefore observed that the ZnZrCa sample maintained two time constants throughout the entire immersion period, indicating that the same general electrochemical mechanism was maintained. Meanwhile, for ZrZnCa, the capacitive contributions and transport processes reorganized during exposure, and after 90 days it exhibited the most favorable electrochemical behaviour of all three samples analysed. In the case of the CaZrZn sample, the initial response was predominantly capacitive; however, after 60 days, it became necessary to include a Warburg contribution, indicating a greater involvement of ionic transport. The results show that the stability of Zn-, Zr- and Ca- based phosphate conversion layers cannot be accurately assessed from a single measurement, and long-term EIS monitoring allows the progressive changes in the layer and at the interface with the corrosive environment to be highlighted.

Keywords: *EIS, Dulbecco, conversion coatings, Ti6Al4V, immersion time.*

Introduction

The evaluation of a coating intended to modify the surface of a metallic implant should not be limited to its electrochemical behaviour immediately after deposition. Prolonged contact with a physiological environment may gradually alter the structure of the interface, may facilitate the penetration of electrolyte through the pores or discontinuities in the coating, and may alter the mechanisms that control charge transfer and ion transport. In the case of the Ti6Al4V alloy, electrochemical stability is largely attributed to the passive oxide layer that forms spontaneously on the surface; however, even this system changes over time when exposed to phosphate-buffered solutions. Gudić et al. demonstrated, through electrochemical impedance spectroscopy measurements carried out in phosphate-buffered solution, that the response of the titanium alloy Ti6Al4V can be described by distinct contributions from the porous outer layer and the internal barrier, and that their properties change with exposure time [1]. This aspect becomes all the more important when the surface of the alloy is coated with an additional layer, the structure and permeability of which introduce new pathways for interaction with the electrolyte.

*Corresponding author: costica.bejinariu@academic.tuiasi.ro

Phosphate conversion coatings offer an interesting approach in this context, as they are not merely a barrier applied over the substrate, but are formed through chemical reactions directly at the metal–solution interface [2]. The phase composition, crystal morphology and layer continuity can be controlled to a certain extent by the composition of the bath and the process parameters. For example, coatings containing hopeite and scholzite have been obtained on titanium and Ti6Al4V, and altering the pH or temperature of the phosphating solution changes the phase ratio, crystal size and electrochemical characteristics of the surface. [3], [4], [5]. For example, Liu et al. successfully grew scholzite layers directly on Ti and Ti6Al4V, which have a lamellar structure and elicit a favourable biological response from osteoblast-like cells [3]. Meanwhile, other studies have shown that the formation of hopeite and scholzite is sensitive to processing conditions, which makes it possible to adjust the structure of the layer as early as the conversion stage [5].

The incorporation of Zn and Ca into such coatings is of interest not only from the perspective of chemical composition, but also because of the effects these ions may have on surface properties. Zn–Ca–P coatings obtained by chemical conversion on titanium have demonstrated both antibacterial activity and an improvement in osteoblastic function [6]. At the same time, a change in the ratio between the zinc phosphate and calcium-zinc phosphate phases influences the corrosion response, which confirms that the mere presence of phosphates is not sufficient to predict the behaviour of the coating. In a previous study conducted on Ti6Al4V, a Ca–Zn coating resulted in a reduction in corrosion current density and an increase in polarisation resistance in both Ringer's solution and Dulbecco's solution, highlighting the potential of these systems for the electrochemical protection of the alloy [7].

A more recent approach involves the use of multicomponent phosphate systems, in which the ions introduced into the conversion bath not only serve to form new phases, but also alter the morphology of the layer. The addition of Zn to an Sr–Ca–P system has been reported to refine the structure and, at higher concentrations, to induce transformations into Sr–Zn–P-type phases [8]. In another study, Sr–Zn–P layers deposited on titanium influenced both the osteogenic response and the polarisation of macrophages, with the effects being dependent on the morphology and composition of the surface [9]. These results show that the design of a multicomponent phosphate coating should be viewed as a matter of striking a balance between structure, chemistry and interfacial behaviour, and not merely as a means of increasing the amount of phosphate deposited.

Similarly, the introduction of Zr into Zn-based phosphate coatings deposited on Ti6Al4V has been shown to significantly alter the surface morphology. In the Zn–Zr layers, in addition to hopeite and phosphophyllite, Zr-bearing phases were identified, and the presence of zircon favoured the formation of a more compact structure. Corrosion behaviour in Ringer's and Dulbecco's solutions was also improved compared with other phosphate compositions investigated [10]. Combining Zn, Ca and Zr within a single system may therefore be of interest, as it allows the production of layers in which the formation of Zn and Ca phosphates is accompanied by structural changes induced by Zr.

However, the initial characterisation of a layer does not provide all the information needed to estimate its stability. Much of the research into phosphate coatings on titanium focuses on phase formation, morphology, adhesion, biological response or electrochemical behaviour at a specific point in time [3], [6], [8], [10]. There is few information available on how the electrochemical processes associated with these layers redistribute themselves following successive periods of immersion. A temporary decrease in impedance does not necessarily imply ongoing degradation, just as any subsequent increase cannot automatically be attributed to the restoration of the original layer. In environments containing phosphates, the surface may change as a result of electrolyte penetration, alterations to interfacial products, and precipitation or dissolution processes; the response measured at a given moment represents the cumulative result of these phenomena [11]. Electrochemical impedance spectroscopy (EIS) is suitable for this type of analysis as it allows the processes taking place over different time scales to be monitored without significantly

disturbing the system. Nyquist and Bode diagrams can highlight the separation or overlap of several time constants, changes in the capacitive behaviour of the layer, and the emergence of contributions associated with mass transport. The use of equivalent electrical circuits then makes it possible to track how these processes change during immersion. In this case, the choice of circuit must be aligned with the experimental shape of the spectra and the physical significance of the elements introduced, as a low value of the statistical fit parameter does not, on its own, guarantee that the chosen model accurately represents the actual interface. Electrochemical studies on titanium and phosphate coatings have shown that responses with two time constants or with additional contributions associated with transport may occur when the surface is inhomogeneous or permeable to the electrolyte [1], [12].

Based on these considerations, the present study investigates the long-term behaviour of three phosphate conversion layers based on Zn, Zr and Ca deposited on Ti6Al4V, using Dulbecco's phosphate-buffered solution (DPBS) as the immersion medium. The electrochemical behaviour was analysed after 30, 60 and 90 days using EIS, with a focus on changes in the Nyquist and Bode plots and on the evolution of the mechanisms described by the equivalent electrical circuits. By comparing the three compositions at successive time intervals, the study aims to highlight not only the differences between the layers, but also how each layer's response reorganises itself during prolonged exposure. This approach thus allows for a more realistic assessment of electrochemical stability than one based solely on characterisation immediately after the layer has been formed.

Materials and Methods

Ti6Al4V alloy specimens were used for the deposition of phosphate conversion coatings. Prior to the phosphating treatment, the surface of the specimens was mechanically prepared by successive sanding with SiC abrasive paper up to grit size 1000. After cleaning, the specimens underwent a surface activation stage, followed by the chemical conversion treatment.

Three variants of Zn-, Zr- and Ca-based phosphating baths were analysed, designated ZnZrCa (with a higher concentration of Zn in solution), ZrZnCa (with a higher concentration of Zr in solution) and CaZrZn (with a higher concentration of Ca in solution). The phosphating solutions had different compositions in terms of the proportions of Zn, Zr and Ca, whilst the other process parameters were kept constant. The phosphating treatment was carried out for 60 minutes at a temperature of approximately 95 °C. At the end of the treatment, the samples were removed from the phosphating bath, rinsed to remove loosely adhering residues and dried prior to further testing.

The behaviour of the layers over time was monitored by immersion in DPBS. Three exposure periods were analysed: 30, 60 and 90 days. Separate samples were used for each period. The samples corresponding to the 30 day interval were removed at the end of this period, whilst the samples intended for the 60 and 90 day assessments remained in the immersion medium until the specified duration was reached. In this way, the samples were continuously exposed throughout the entire period corresponding to each analysis interval. After each immersion period, the electrochemical behaviour of the coatings was assessed using electrochemical impedance spectroscopy.

EIS measurements were carried out using an OrigaFlex OGF+01A electrochemical system (Sudelec, France). Prior to each measurement, the samples were held at open-circuit potential for 60 minutes to stabilise the electrochemical response.

The EIS spectra were recorded in the frequency range 100 kHz to 0.01 Hz, using a sinusoidal signal amplitude of 10 mV and 10 data points per decade of frequency and the exposed surface was 0.283 cm^2. The measurements were taken after 30, 60 and 90 days of immersion in DPBS. The experimental data were analysed using Nyquist and Bode plots, and modelling with equivalent electrical circuits was carried out using the ZSimWin software.

Results and Discussions

The ZnZrCa sample after 30 days of immersion

After 30 days of immersion in DPBS, the Nyquist plot of the ZnZrCa sample (Fig. 1) shows a broad capacitive response, without the arc closing completely within the investigated frequency range. At low frequencies, the imaginary component of the impedance continues to increase, indicating that the dominant electrochemical process is not fully confined down to the lower limit of 0.01 Hz.

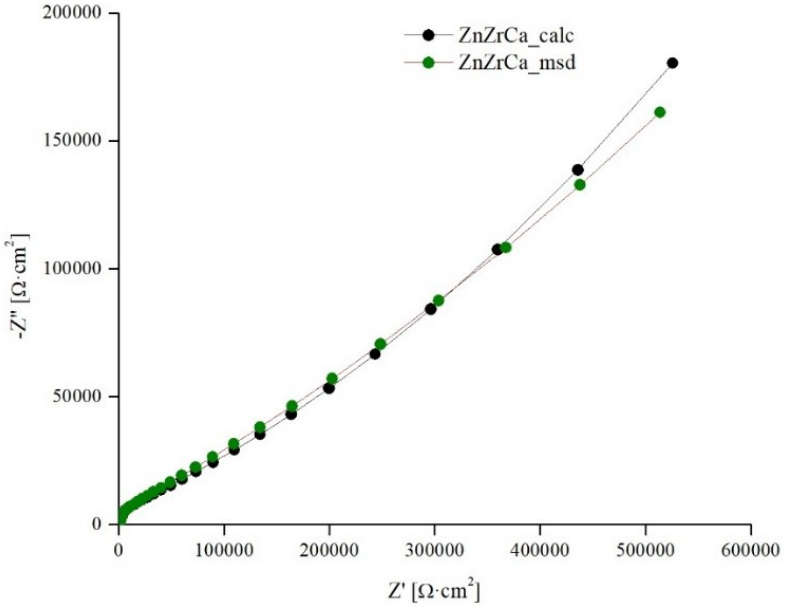

Fig. 1. The experimental Nyquist plot and the curve obtained by fitting for the ZnZrCa layer after 30 days of immersion in DPBS

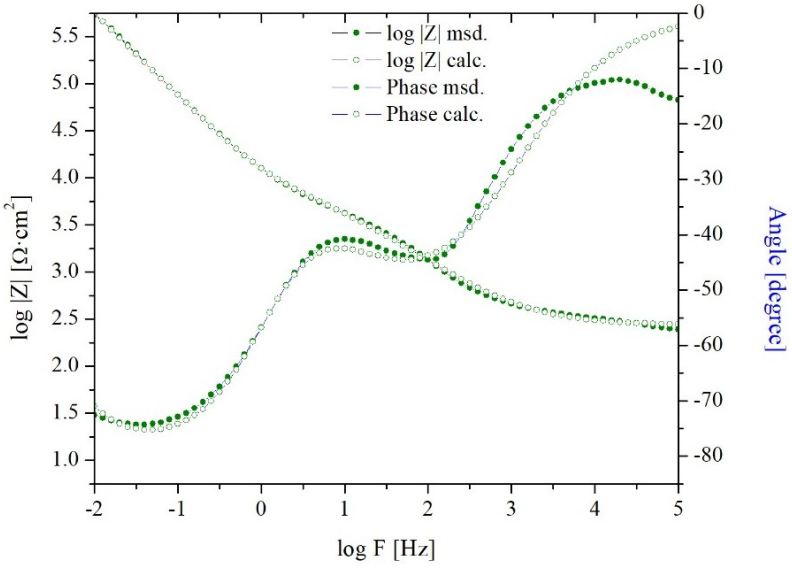

Fig. 2. Experimental Bode plot and the curve obtained by fitting for the ZnZrCa layer after 30 days of immersion in DPBS

The same trend is evident in the Bode plot (Fig. 2), where the magnitude of the impedance increases progressively as the frequency decreases. The phase angle exhibits a broad peak of approximately 74º in the low-frequency range, whilst a second, less pronounced contribution is observed in the intermediate frequency region. The shape of the curve thus indicates the presence of two relaxation processes that partially overlap.

The spectrum was modelled using the equivalent electrical circuit R(QR)(QR), Fig. 3. In this configuration, the solution resistance, R_s, represents the ohmic contribution of the electrolyte, whilst the two QR branches describe two electrochemical processes characterised by different time constants. The constant-phase elements, $Q_1 = 2.01 \cdot 10^{-5}\ S \cdot s^n/cm^2$ and $Q_2 = 1.46 \cdot 10^{-5}\ S \cdot s^n/cm^2$, were used in place of ideal capacitors because the surface response is not perfectly capacitive. Such a deviation is to be expected for a phosphate conversion coating, the structure of which may exhibit morphological irregularities, local variations in composition and a non-homogeneous distribution of electrical properties.

For this fit, the first branch is characterised by $n_1=0.88$, a value relatively close to 1, which indicates a predominantly capacitive response, though still not ideal. The second branch exhibits a lower exponent, $n_2=0.64$, indicating a more pronounced dispersion of the time constants. This difference suggests that the two contributions originate from electrochemical regions with different degrees of heterogeneity.

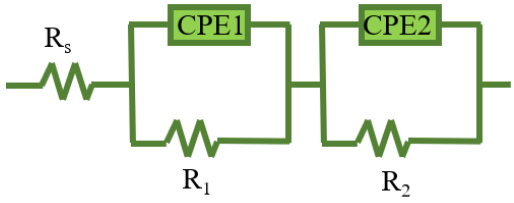

Fig. 3. The equivalent electrical circuit used to model the EIS spectra of ZnZrCa after 30, 60 and 90 days of immersion in DPBS

From a physical point of view, the circuit may be associated with the response of the phosphate layer and with the processes taking place at the interface between the layer, the electrolyte and the substrate. The process observed at higher frequencies may be linked to the layer's response and the penetration of the electrolyte through its pores or defects, whilst the low-frequency process reflects slower phenomena taking place in the interfacial region.

The values obtained for the two resistances are approximately $R_1=3.94 \cdot 10^6\ \Omega \cdot cm^2$ and $R_2=5.83 \cdot 10^3\ \Omega \cdot cm^2$. The value of the R_1 indicates high resistance to the corresponding electrochemical process. This high value is consistent with the pronounced capacitive response observed at low frequencies and with the fact that the Nyquist plot does not close within the measured range. The R_2 is several orders of magnitude smaller than that associated with the slow process, which shows that this contribution offers much less resistance to charge transport or ion movement through the accessible regions of the layer.

The large difference between the two resistances, together with the distinct values of the CPE exponents (Q and n), indicates that after 30 days, the layer does not behave as a uniform electrochemical barrier. One part of the system retains a strongly capacitive character and high resistance, whilst a second contribution is associated with more heterogeneous regions that are more readily accessible to the electrolyte. This combination is consistent with the characteristic structure of a phosphate conversion layer, in which compact regions coexist with pores, grain boundaries and other local discontinuities.

The value $\chi^2=6.69 \cdot 10^{-3}$ supports the use of the R(QR)(QR) circuit to describe the electrochemical response of the ZnZrCa sample after 30 days of immersion in DPBS.

The ZnZrCa sample after 60 days of immersion

After 60 days of immersion in DPBS, the Nyquist plot (Fig. 4) retains a predominantly capacitive response, although the arc is not completely bounded within the investigated frequency range. As the frequency decreases, both the real component (Z') and the imaginary component of the impedance (–Z'') continue to rise. At 0.01 Hz, the values are approximately 12.27 kΩ·cm^2 for Z' (the real component) and 18.97 kΩ·cm^2 for –Z'' (imaginary component), which corresponds to an impedance modulus of approximately $2.26 \cdot 10^4$ Ω·cm^2. The fact that the arc does not close completely indicates that the slow electrochemical process continues beyond the lower frequency limit used in the experiment.

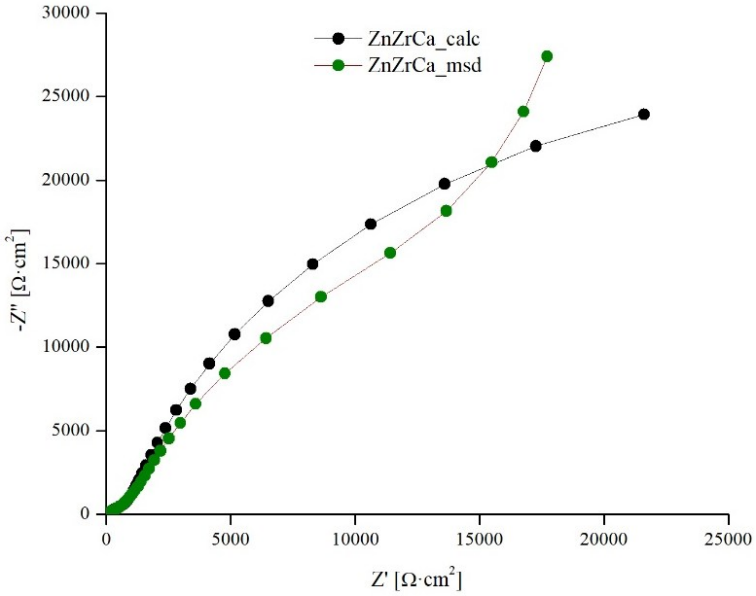

Fig. 4. The experimental Nyquist plot and the curve obtained by fitting for the ZnZrCa layer after 60 days of immersion in DPBS

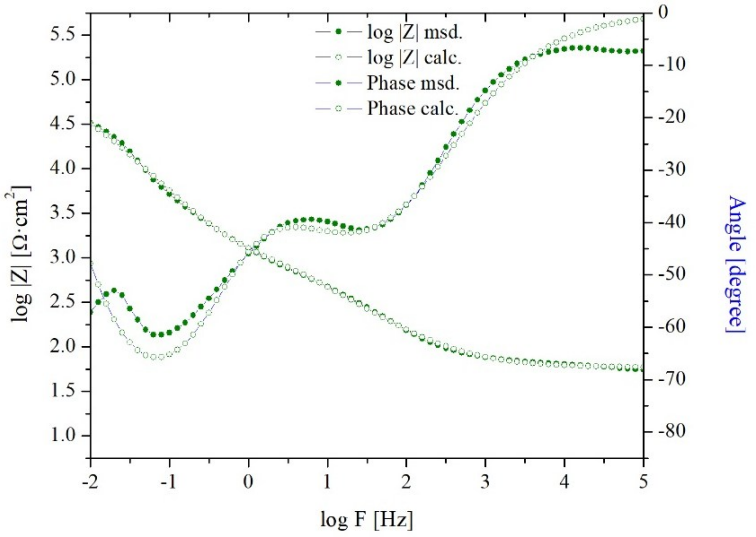

Fig. 5. Experimental Bode plot and the curve obtained by fitting for the ZnZrCa layer after 60 days of immersion in DPBS

The Bode plot (Fig. 5) confirms the complex nature of the response. The phase angle increases at low frequencies and reaches approximately 61º at around 0.06 Hz, after which it decreases towards the intermediate frequency range. In this region, there is a broad band in which the phase angle remains around 41º, highlighting the contribution of a second relaxation process. Consequently, the spectrum cannot be described by a single time constant. The two contributions are partially superimposed, but remain sufficiently distinct to justify the use of two capacitive-resistive branches.

The modelling was carried out using the equivalent circuit R(QR)(QR), the same type of circuit that describes the presence of two non-ideal electrochemical processes (Fig. 3). In this case, the solution resistance, R_s, was 58.52 Ω·cm². The two QR branches describe responses with different dynamics, and the use of constant-phase elements in place of ideal capacitors is justified by the non-uniform nature of the phosphate layer and the interfaces developed during immersion.

The slow process is characterised by $Q_1=2.79\cdot10^{-4} S\cdot s^n/cm^2$ and by an exponent $n_1=0.88$. The value of n_1, which is relatively close to unity, shows that this contribution remains predominantly capacitive. The deviation from the ideal value (n=1) does, however, indicate that the response does not originate from a perfectly homogeneous interface. In the case of a phosphate layer, this behaviour may reflect a non-uniform thickness distribution, surface roughness, boundaries between crystals, and non-uniform electrolyte access across different regions of the layer.

The resistance associated with this process is $R_1=6.21\cdot10^4 \Omega\cdot cm^2$. Of the circuit's two resistive contributions, this is by far the dominant one and indicates that the slow process still encounters significant electrochemical resistance after 60 days of contact with DPBS. The location of this time constant in the very low-frequency range suggests that it is related more to phenomena occurring deep within the layer–substrate system and in the regions accessible to the electrolyte after it has passed through the layer, rather than to a purely surface-level response.

The second branch is characterised by $Q_2=1.59\cdot10^{-4}\ S\cdot s^n/cm^2$and by a lower exponent, $n_2=0.63$. The value shows a much more dispersed response than that corresponding to the slow process. This dispersion indicates the existence of a wider range of time constants and may be linked to the heterogeneous nature of the layer, the pores and the preferential pathways through which the electrolyte interacts with the surface. The resistance corresponding to this contribution is $R_2=977\ \Omega\cdot cm^2$, which is much lower than the value of R_1. This difference shows that the two processes do not contribute equally to the total impedance of the system; one is highly resistive and slow, whilst the other is characterised by lower resistance and a much less ideal capacitive response.

The difference between $n_1$and n_2, together with the difference of nearly two orders of magnitude between the two resistances, supports the idea of a non-uniform electrochemical layer, in which more resistive regions coexist with areas through which the electrolyte can penetrate and interact more easily with the substrate.

There is good agreement between the experimental and calculated data; the value χ^2 being $5.49\cdot10^{-3}$.

The ZnZrCa sample after 90 days of immersion

The Nyquist plot (Fig. 6) shows that a predominantly capacitive response is maintained, with the low-frequency component not being completely suppressed after 90 days of immersion. At 0.01 Hz, Z' reaches ~34.74 kΩ·cm², and –Z" at ~27.51 kΩ·cm², resulting in an impedance modulus of approximately $4.43\cdot10^4\ \Omega\cdot cm^2$. Compared with the value recorded after 60 days, the low-frequency impedance increases again. However, it remains below the level observed after 30 days, which indicates that the electrochemical behaviour of the layer is not consistent throughout the 90-day exposure period.

The Bode plot (Fig. 7) highlights more clearly the separation of the processes contributing to this response. The phase angle reaches a maximum of approximately 70º, and in the low-frequency range remains around ~40º, without returning to zero until 0.01 Hz. The shape of the

curve, together with the change in the slope of the impedance modulus, indicates the persistence of two electrochemical contributions with different time constants. Compared with 60 days, the position and relative intensity of these contributions change, but no new element emerges that would necessitate a change in the architecture of the equivalent circuit.

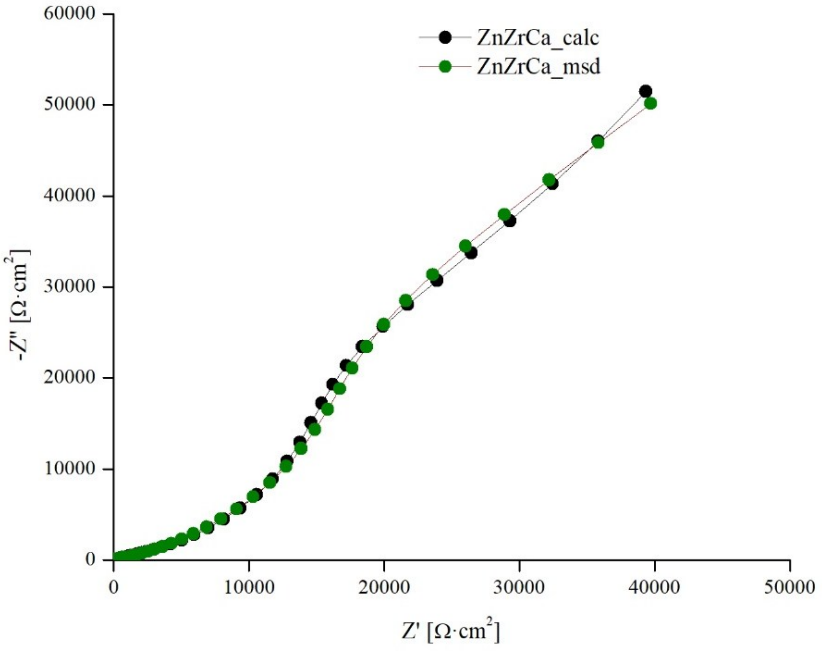

Fig. 6. The experimental Nyquist plot and the curve obtained by fitting for the ZnZrCa layer after 90 days of immersion in DPBS

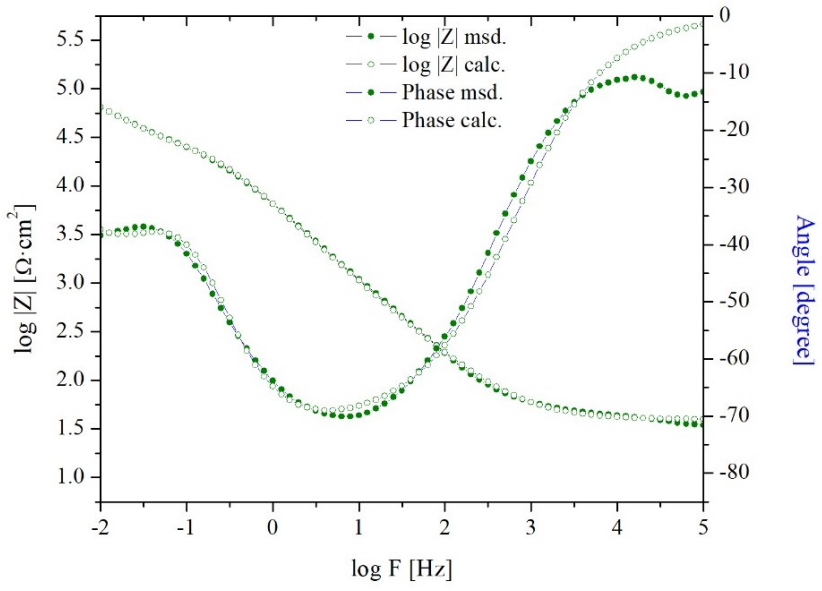

Fig. 7. Experimental Bode plot and the curve obtained by fitting for the ZnZrCa layer after 90 days of immersion in DPBS

For this reason, the spectrum was further described by the R(QR)(QR) circuit, Fig. 3. Maintaining the same circuit at 30, 60 and 90 days is important because it shows that, for the ZnZrCa sample, the general structure of the electrochemical response remains the same throughout the immersion period. The changes observed over time are reflected primarily in the parameter values of the two branches, rather than in the emergence of an additional mechanism that would require a different type of circuit.

Therefore, the R_s value is 39.15 $\Omega \cdot cm^2$. Meanwhile, the first relaxation contribution is characterised by $Q_1=1.05 \cdot 10^{-4}$ $S \cdot s^n/cm^2$ and an exponent $n_1=0.68$. The relatively low value of n_1 indicates a highly dispersed response, characteristic of a non-uniform electrochemical region. After 90 days, this contribution may be linked to the existence of multiple transport pathways and the non-uniform distribution of electrical properties within the layered system–electrolyte–substrate, without the surface being able to be treated as an ideal capacitive interface.

The resistance associated with this contribution amounts to $R_1=1.88 \cdot 10^5$ $\Omega \cdot cm^2$. This high value indicates that the slow process still encounters significant electrochemical resistance after 90 days. At the same time, the fact that the low-frequency response is not fully confined within the measured range suggests that this contribution develops over a timescale longer than that fully covered by the experiment. Consequently, the main significance of this value is that the system retains a pronounced slow resistive component, not merely a superficial response of small amplitude.

The second branch exhibits different behaviour. For this, the following values were obtained: $Q_2=4.52 \cdot 10^{-5}$ $S \cdot s^n/cm^2$ and $n_2=0.91$. The value of the exponent is much closer to 1 than in the case of the first branch and indicates a more clearly defined capacitive response. The associated resistance is $R_2=1.\ 59 \cdot 10^4 \Omega \cdot cm^2$, which is lower than R_1, but sufficiently high to show that this region contributes significantly to the overall response of the layer. The association between n_2 and R_2 suggests the existence of a component of the system that behaves more uniformly from an electrochemical point of view than the region described by the CPE1.

The difference between the values of n_1 and n_2 shows that the two branches do not merely represent processes with different resistances, but also regions with different degrees of electrochemical uniformity. One of the contributions is highly dispersed and associated with a slow process, whilst the other retains an almost capacitive character. These values suggest that, even after 90 days in the DPBS, the layer still exhibits regions with distinct electrochemical behaviour.

The trend over the 90-day period fluctuates. Thus, the impedance modulus at 0.01 Hz falls sharply between 30 and 60 days, after which it rises again at 90 days. At the same time, the CPE exponent values show that the two types of response – one more akin to capacitive behaviour and one highly dispersed – persist throughout the entire period, even though their relative proportions change. Thus, the results do not indicate a simple progressive loss of electrochemical properties, but rather an evolution and reorganisation of the interfacial response during immersion.

The R(QR)(QR) model satisfactorily reproduces both the Nyquist plot and the behaviour of the impedance modulus and phase angle, yielding a value of $\chi 2 = 6.87 \cdot 10^{-3}$.

The ZrZnCa sample after 30 days of immersion

For the ZrZnCa sample, the electrochemical response recorded after 30 days has a clear capacitive component. However, its behaviour at low frequencies can no longer be described solely by a capacitive arc. In the Nyquist plot (Fig. 8), the curve remains open and tends towards an almost linear trend at the far end of the spectrum. At 0.01 Hz, Z' reaches ~25.39 $k\Omega \cdot cm^2$, and –Z'' reaches ~28.97 $k\Omega \cdot cm^2$. The similar values of the two components and the orientation of the trajectory in this region suggest that species transport begins to contribute significantly to the electrochemical response.

This characteristic can also be seen in the Bode plot (Fig. 9). The impedance modulus increases continuously as the frequency decreases, from ~20.6 Ω·cm^2 at 100 kHz to ~3.85·10^4 Ω·cm^2 at 0.01 Hz. The phase angle curve exhibits a broad peak of ~65.6º, around a frequency of 25 Hz, indicating the presence of a significant capacitive contribution. Towards the low-frequency range, the phase decreases but does not approach zero. At 0.01 Hz, it remains at around ~49º. It is precisely this behaviour, together with the shape of the terminal portion of the Nyquist plot, that justified the inclusion of a Warburg element in the equivalent model.

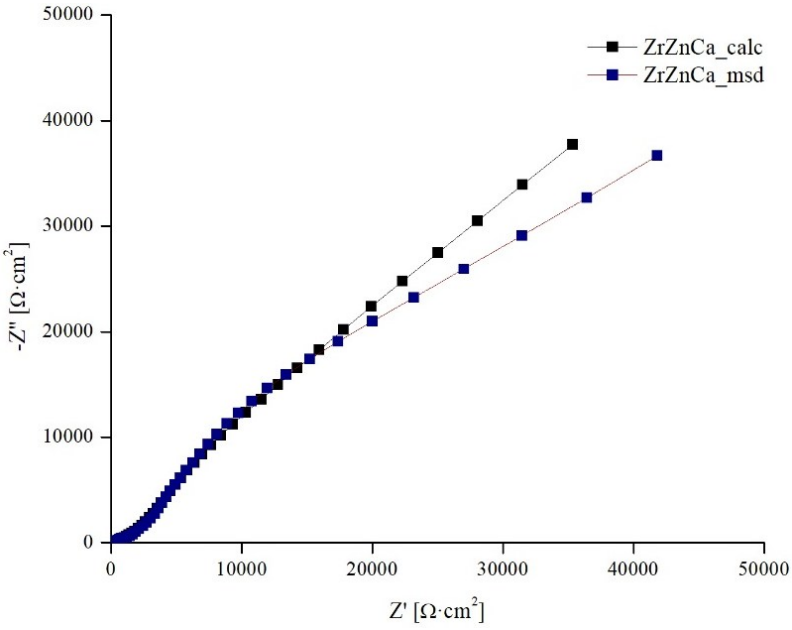

Fig. 8. The experimental Nyquist plot and the curve obtained by fitting for the ZrZnCa layer after 30 days of immersion in DPBS

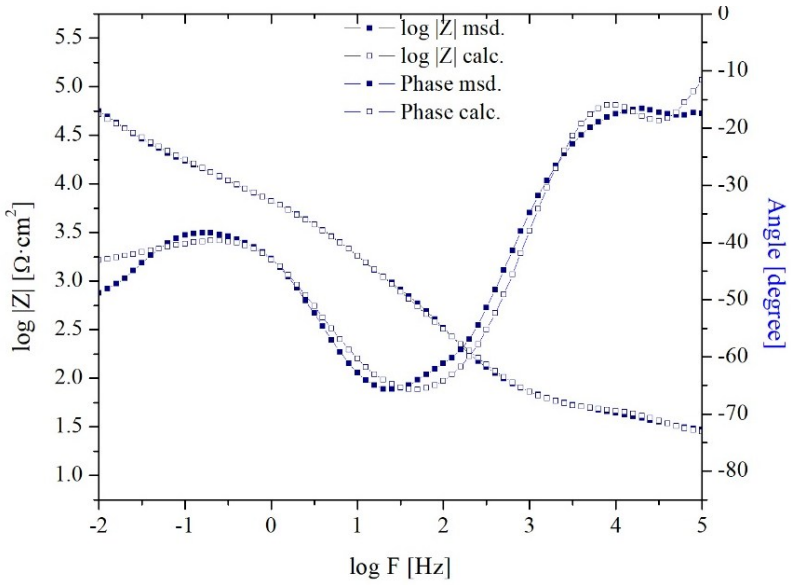

Fig. 9. Experimental Bode plot and the curve obtained by fitting for the ZrZnCa layer after 30 days of immersion in DPBS

The circuit that best describes the spectrum is R(Q(RW))(CR), Fig. 10. The value of R_s is 26.12 $\Omega \cdot cm^2$ and corresponds to the ohmic contribution of the medium and the electrochemical cell. The main answer, however, lies in the Q(RW) branch, in which the non-ideal capacitive behaviour is coupled with a resistance and a transport dependent component.

The constant-phase element (CPE) has $Q=1.59 \cdot 10^{-5}$ $S \cdot s^n/cm^2$ and n = 0.83. This indicates behaviour that remains predominantly capacitive but is sufficiently far from the ideal case to reflect the layer's non-uniform nature. In a phosphate conversion layer, such variation may arise from local differences in thickness, roughness or porosity, or from the non-uniform distribution of crystals and areas accessible to the electrolyte. The resistance of this branch is $R_1=6.20$ $k\Omega \cdot cm^2$, which indicates that the main process encounters significant electrochemical resistance. At the same time, the value of the Warburg parameter, $W=7.82 \cdot 10^{-5}$ $S \cdot s^{0.5}/cm^2$, indicates that the low-frequency response is not governed solely by the capacitive and resistive properties of the interface. Ion transport through the permeable zones of the layer or towards deeper regions of the interface is already contributing to the system's behaviour after 30 days of immersion.

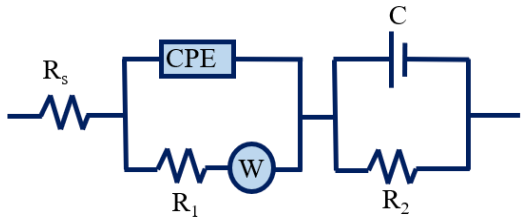

Fig. 10. The equivalent electrical circuit used to model the EIS spectra of ZrZnCa after 30 and 90 days of immersion in DPBS and of CaZrZn after 30 days of immersion in DPBS

The CR branch introduces a much faster response. Its capacitance is $C=3.18 \cdot 10^{-7}$ F/cm^2, and the associated resistance is only $R_2=18.63$ $\Omega \cdot cm^2$. Compared with R_1, this contribution accounts for a small resistive component of the overall response. This may be linked to a rapid process occurring at the layer/substrate interface.

In the case of the ZrZnCa sample, the presence of the Warburg element distinguishes its response from that of a coating which behaves exclusively as a capacitive barrier. After 30 days, even though the layer continues to provide significant protection, the electrolyte gains access to pathways through which ion transport becomes significant. This combination of the capacitive nature of the layer and the transport contribution explains the distinctive shape of the Nyquist and Bode plots.

The model reproduces the experimental data well, with a value of $\chi^2=3.50 \cdot 10^{-3}$. In this case, the choice of the R(Q(RW))(CR) circuit is supported not only by the quality of the fit, but above all by the experimental behaviour in the low-frequency range.

The ZrZnCa sample after 60 days of immersion

After 60 days of immersion, the response of the ZrZnCa sample differs from that observed at 30 days, particularly in the low-frequency range. The Nyquist plot (Fig. 11) does not show a closed semicircle, but rather a continuous trend towards high impedance values. At 0.01 Hz, Z' reaches ~25.31 $k\Omega \cdot cm^2$, and –Z'' reaches ~22.54 $k\Omega \cdot cm^2$. The corresponding impedance modulus is ~$3.39 \cdot 10^4$ $\Omega \cdot cm^2$. The curve's slope changes noticeably in the low-frequency region, indicating that the response cannot be attributed to a single capacitive process.

The Bode plot (Fig. 12) shows that the phase angle rises to a maximum of ~66.8º, occurring at around 16 Hz, after which it gradually decreases. In the low-frequency range, however, this

decrease does not continue towards zero. After a minimum of ~29º at around 0.2 Hz, the phase angle increases again and reaches ~41.7º at 0.01 Hz. This rebound indicates the presence of an additional slow component, which only becomes apparent towards the lower limit of the investigated range. At the same time, the impedance modulus increases from ~16.6 $\Omega \cdot cm^2$ at 100 kHz to nearly $3.4 \cdot 10^4$ $\Omega \cdot cm^2$ at 0.01 Hz.

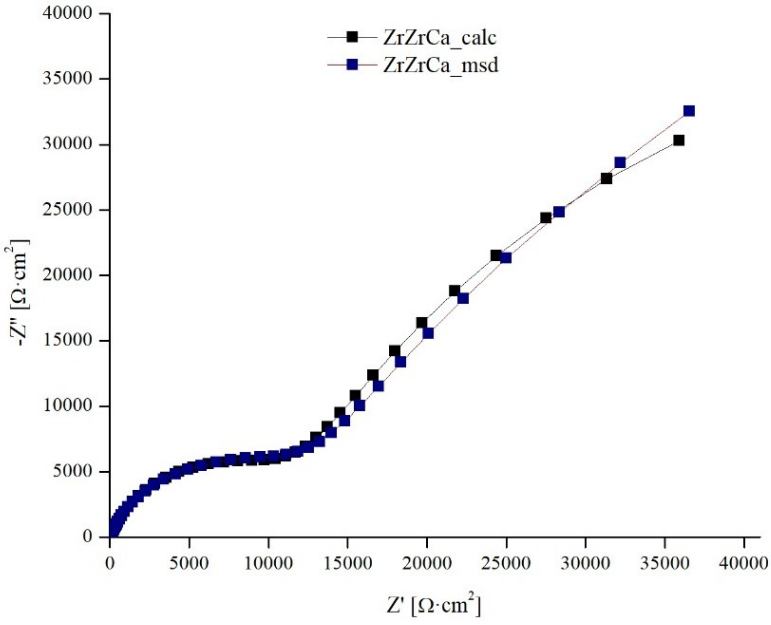

Fig. 11. The experimental Nyquist plot and the curve obtained by fitting for the ZrZnCa layer after 60 days of immersion in DPBS

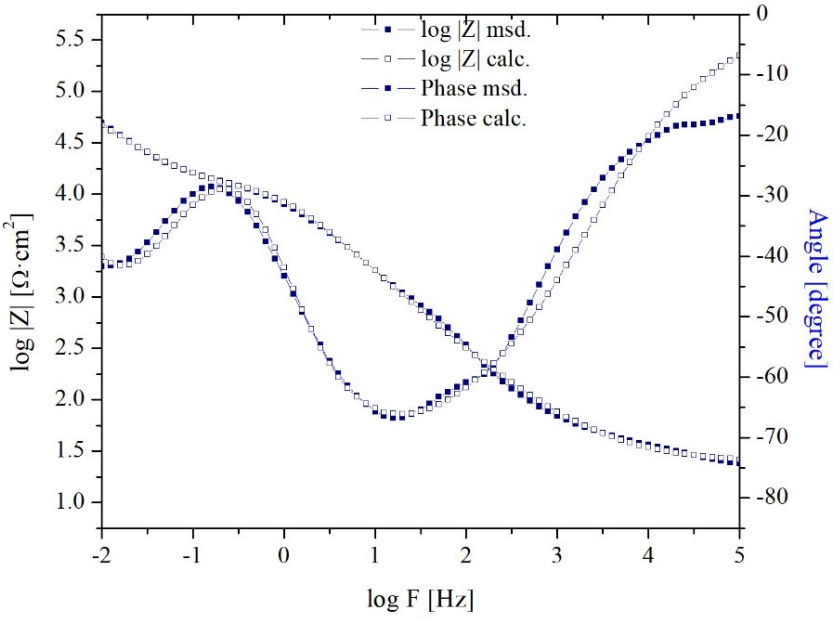

Fig. 12. Experimental Bode plot and the curve obtained by fitting for the ZrZnCa layer after 60 days of immersion in DPBS

For this spectrum, the most suitable representation was obtained using the R(QR)(QR)W circuit, Fig. 13. Unlike the 30-day response, where the Warburg contribution could be incorporated into the dominant electrochemical process, after 60 days, the two relaxations are more clearly distinguished, and the transport contribution appears separately in the low-frequency range. This change in the circuit may be due to a change in the weighting and separation of the processes that contribute to the total impedance.

In this case, R_s is 23.36 $\Omega \cdot cm^2$, so the overall response is governed primarily by the processes associated with the layer and the interface, rather than by the resistance of the electrolyte. The first QR branch gives $Q_1=2.99 \cdot 10^{-4}$ $S \cdot s^n/cm^2$ and $n_1=0.85$. The exponent is relatively close to 1, indicating a predominantly capacitive contribution, but with sufficient dispersion to reflect the non-uniformity of the surface. The resistance associated with this branch (R_1) is ~$6.36 \cdot 10^4$ $\Omega \cdot cm^2$, the largest of the circuit's resistive contributions. Consequently, this process represents the system's main electrochemical barrier at 60 days.

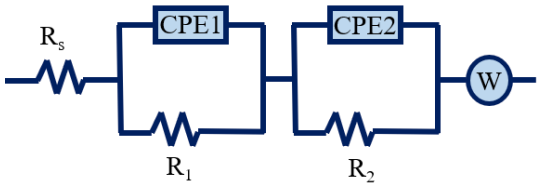

Fig. 13. The equivalent electrical circuit used to model the EIS spectra of ZrZnCa after 60 days of immersion in DPBS

The second branch has a value of $Q_2=1.92 \cdot 10^{-5}$ $S \cdot s^n/cm^2$ which is smaller, and the exponent $n_2=0.87$ indicates that this process also retains a fairly well-defined capacitive character. The corresponding resistance (R_2), of approximately $9.97 \cdot 10^3$ $\Omega \cdot cm^2$, is considerably lower than that of the first branch. The two values of n are close to one another, which suggests that at 60 days both capacitive contributions originate from regions with comparable degrees of non-ideality, even though their resistive opposition is very different.

This situation differs from that observed after 30 days, when the response was dominated by a single CPE component associated with transport and a rapid CR-type process. After 60 days, the two capacitive contributions can be distinguished more clearly, which may reflect a reorganisation of the interface during prolonged exposure. The electrolyte probably does not interact with the layer in the same way across all regions, and the evolution over time may lead to a differentiation between the response of the layer itself and that of deeper or more ionically accessible regions.

To these is added the Warburg term, with a value of $W=3.38 \cdot 10^{-4}$ $S \cdot s^{0.5}/cm^2$. Its presence is consistent with the phase angle returning to ~42º at very low frequencies and with the open-loop shape of the Nyquist plot. Thus, after 60 days, the transport of species through the layer or towards the interface remains a significant component of the electrochemical response. However, this is not a system controlled exclusively by diffusion; the Warburg component coexists with two well-defined capacitive-resistive processes.

The results obtained describe a system in which the main resistive barrier remains significant, but the response is split between two distinct electrochemical regions and a transport contribution at low frequencies. This structure explains both the Nyquist shape and the unusual evolution of the phase angle in the lower part of the spectrum.

For the circuit R(QR)(QR)W, the following was obtained $\chi^2=8.04 \cdot 10^{-3}$. Although this value is higher than that obtained at 30 days, the choice of circuit is supported by the experimental spectrum's shape.

The ZrZnCa sample after 90 days of immersion

At 90 days, the ZrZnCa sample does not continue the trend observed at 60 days. On the contrary, the low-frequency response becomes much more pronounced once again, and the spectrum can be described using the same circuit configuration as that used at 30 days, R(Q(RW))(CR). This return to the same topology suggests that the dominant electrochemical processes are similar to those identified during the initial immersion stage, although their intensity has changed considerably in the meantime.

The difference is evident from the Nyquist plot, Fig. 14. At 0.01 Hz, Z' reaches ~72.5 kΩ·cm^2, and –Z'' reaches ~51.9 kΩ·cm^2, values that are much higher than those recorded after 60 days. The impedance modulus thus reaches ~8.92·10^4 Ω·cm^2, compared with ~3.4·10^4 Ω·cm^2 at 60 days. This increase does not necessarily indicate structural recovery of the layer, but it clearly shows that after 90 days the system once again exhibits greater electrochemical resistance to processes occurring at low frequencies. The evolution is therefore non-linear: the response changes at 60 days, and subsequently the interface reaches a different electrochemical state.

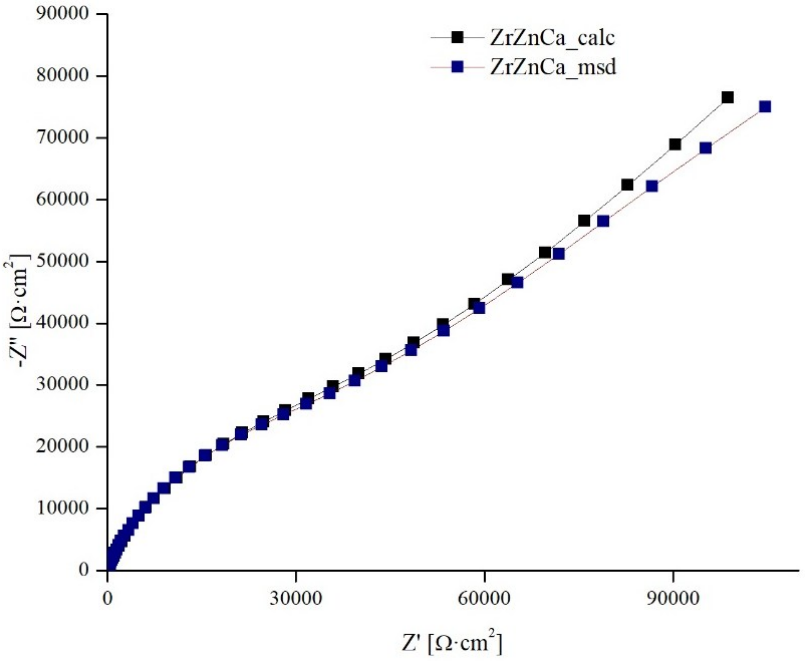

Fig. 14. The experimental Nyquist plot and the curve obtained by fitting for the ZrZnCa layer after 90 days of immersion in DPBS

The Bode plot (Fig. 15) also supports this change. The peak phase angle is ~67.6º, around a frequency of 20 Hz, which highlights a clearly defined capacitive contribution. Towards lower frequencies, the phase decreases gradually, but remains at ~35.6º at 0.01 Hz. At the same time, the impedance modulus continues to increase, without reaching a final plateau. This combination indicates that the slow process is not purely resistive and that species transport continues to influence the interface response.

The R(Q(RW))(CR) circuit captures this behaviour through a main process, described by the Q(RW) branch, and a faster contribution, represented by CR. R_s is 32.04 Ω·cm^2, whilst the constant-phase element has Q = 1.24·10^{-5} S·s^n/cm^2 and n = 0.78. The value of the exponent confirms that the dominant process remains capacitive, but it is further from the behaviour of an ideal capacitor than would be the case for a uniform surface. After 90 days, the layer and the

interface must therefore be regarded as a heterogeneous system, in which different regions respond on similar, but not identical, time scales.

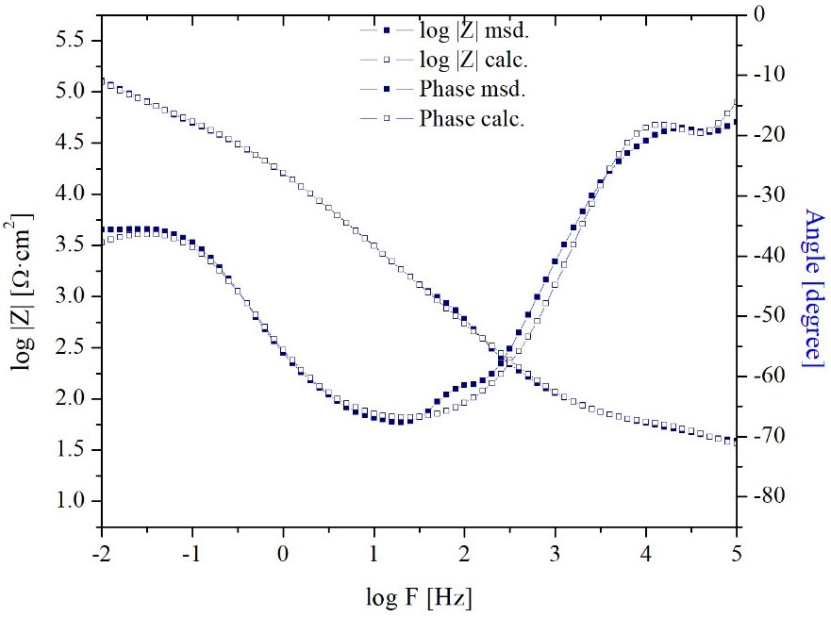

Fig. 15. Experimental Bode plot and the curve obtained by fitting for the ZrZnCa layer after 90 days of immersion in DPBS

The resistance associated with this branch is $R_1 = 4.89 \cdot 10^4\ \Omega \cdot cm^2$. This constitutes the main resistive contribution to the circuit and is consistent with the high impedance observed experimentally at low frequencies. Compared with the value of approximately 6.20 $k\Omega \cdot cm^2$ obtained at 30 days for the same circuit configuration, the increase is substantial. Within the limits of the model used, the result suggests that the electrochemical process associated with this region of the interface is more strongly impeded following prolonged exposure. However, it is not necessary to attribute this change exclusively to the initial phosphate layer; after 90 days, the contribution of products formed during immersion and changes in the interface chemistry may also contribute to the measured response.

The Warburg component remains necessary, given that $W=3.72 \cdot 10^{-5}\ S \cdot s^{0.5}/cm^2$. Its presence indicates that, despite the increase in resistance, the access and transport of species through the layer or near the interface do not cease. Therefore, the high impedance observed at 90 days does not correspond to a completely impermeable barrier. The response results from the superposition of a strong capacitive-resistive contribution with a transport process that remains active at low frequencies.

The fast process described by the CR branch has a capacitance of $C = 2.09 \cdot 10^{-7}\ F/cm^2$ and $R_2=21.62\ \Omega \cdot cm^2$. The very low value of this resistance, compared with R_1 of the main process, indicates that this contribution does not govern the overall electrochemical protection. Rather, it reflects a local and rapid response of a surface region of the system, whilst the long-term behaviour is dominated by the Q(RW) branch.

The shift from 30 to 60 days and the subsequent return do not necessarily indicate the disappearance and reappearance of the same processes, but more likely a change in their relative proportions and their separation in the frequency domain. At 60 days, two capacitive contributions could be distinguished more clearly, whilst at 90 days, the response is once again dominated by a non-ideal capacitive process directly coupled to species transport.

The model developed for 90 days accurately reproduces the experimental trend, with $\chi^2=2.79\cdot10^{-3}$. In the case of ZrZnCa, the overall picture after 30, 60 and 90 days is thus one of continuous reorganisation of the interface, rather than linear degradation.

The CaZrZn sample after 30 days of immersion

In the case of the CaZrZn sample, the spectrum obtained after 30 days has a different shape to that observed for ZrZnCa. There is no low-frequency broadening to suggest any obvious diffusive control. On the contrary, in the Nyquist plot (Fig. 16), the spectrum begins to curve towards the real axis at the final measured points, which indicates a tendency for the capacitive response to close. At 0.01 Hz, Z' is ~46.07 kΩ·cm^2 , and –Z'' is ~25.86 kΩ·cm^2, corresponding to an impedance modulus of ~$5.28\cdot10^4$ Ω·cm^2. The high impedance at low frequency indicates that, after the first month of exposure, the system retains significant resistance to slow electrochemical processes.

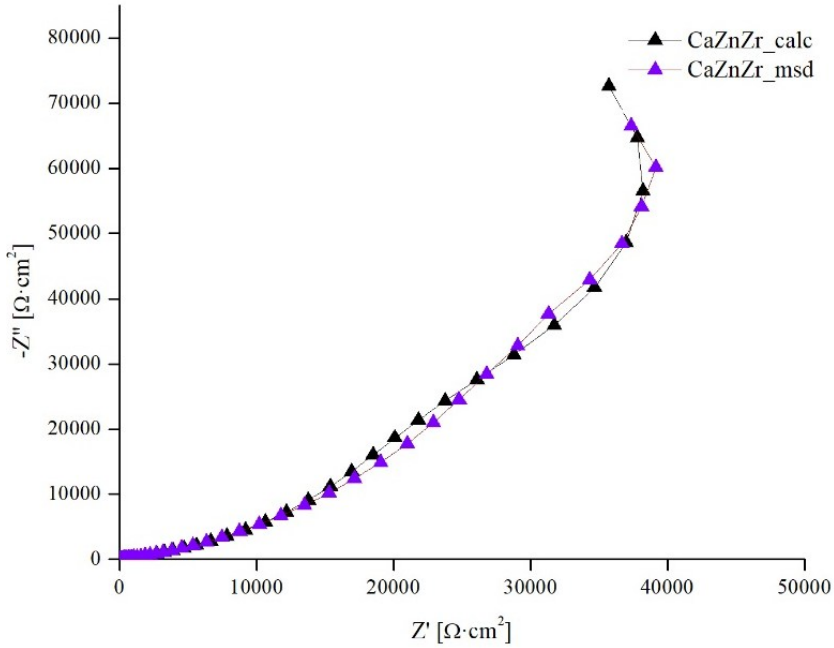

Fig. 16. The experimental Nyquist plot and the curve obtained by fitting for the CaZrZn layer after 30 days of immersion in DPBS

The Bode plot (Fig. 17) is consistent with the previous observations. The impedance modulus increases by more than three orders of magnitude between 100 kHz and 0.01 Hz, from ~13.1 Ω·cm^2 to ~52.8 kΩ·cm^2. The phase angle forms a broad region with high values, peaking at approximately 74º around 8 Hz. The width of this region and the gradual change in slope indicate that the response does not correspond to a single time constant. At very low frequencies, the phase drops to approximately 29º, in parallel with the curvature of the Nyquist plot. No maintenance of the phase near the values associated with a diffusive regime is observed here, which is why the introduction of a Warburg element is not necessary.

For CaZrZn, the spectrum was best described by the R(QR)(CR) circuit, Fig. 18. This includes two capacitive-resistive contributions, but these are not of the same nature. The first is represented by a constant-phase element (CPE), whilst for the second, an ideal capacitor (C) was sufficient to describe the data. This difference suggests that the two electrochemical regions do not exhibit the same degree of heterogeneity.

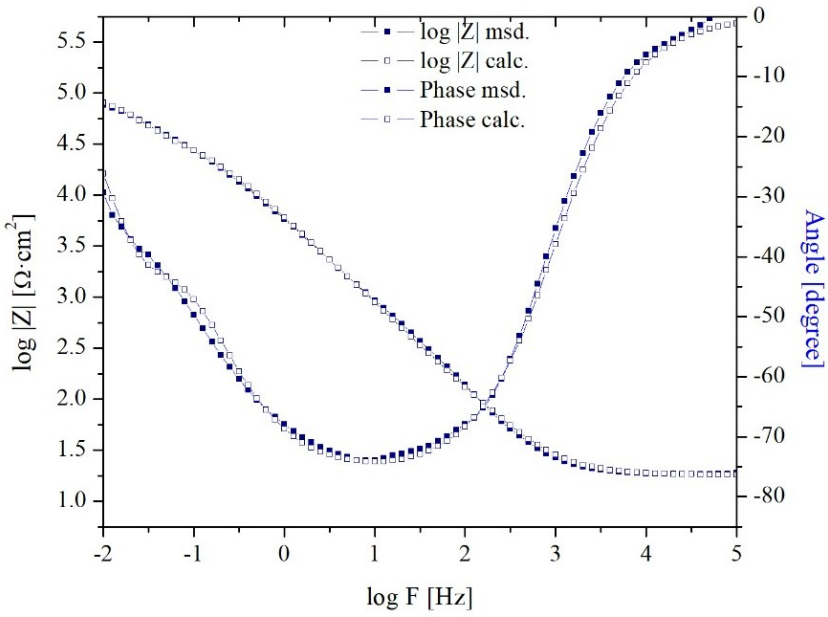

Fig. 17. Experimental Bode plot and the curve obtained by fitting for the CaZrZn layer after 30 days of immersion in DPBS

R_s has a low value of ~18.11 Ω·cm^2, which indicates that most of the measured impedance stems from the layer and interfacial processes, rather than from the electrolytic medium. For the QR branch, the value Q = 3.95·10^{-5} S·s^n/cm^2 is associated with an exponent n = 0.83. This indicates a predominantly capacitive response, but one that is still sufficiently non-ideal to reflect the non-uniformity of the phosphate layer. The distribution of the crystals, the boundaries between them, the roughness and any local pathways for electrolyte penetration may contribute to this deviation from the behaviour of an ideal capacitor.

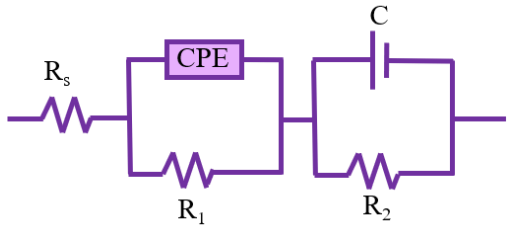

Fig. 18. The equivalent electrical circuit used to model the EIS spectra of CaZrZn after 30 days of immersion in DPBS.

The resistance of this first contribution (R_1) is ~2.90·10^4 Ω·cm^2. This value indicates that the regions described by the QR branch continue to provide a significant electrochemical barrier after 30 days. Taken together with n value, the result suggests a barrier that is not perfectly uniform, but which retains its resistive and capacitive nature.

The second contribution is different. It is characterised by a capacitance C = 1.70·10^{-4} F/cm^2 and a resistance R_2 = 6.87·10^4 Ω·cm^2. The relatively high capacitance and the resistance greater than R_1 are consistent with a slower interfacial process, which becomes significant towards the lower limit of the frequency range. The fact that this component could be represented by an ideal capacitor, rather than by a second CPE, indicates a more well-defined response than that of the region described by the first branch. This does not mean that the interface is perfectly

homogeneous, but merely that the dispersion of the process in question did not necessitate the use of a constant-phase element to reproduce the spectrum.

The two resistances indicate that electrochemical protection is not provided by a single process. One contribution is associated with a layer exhibiting a non-ideal, distributed response, whilst the other is associated with a slower process, featuring a well-defined capacitive component and greater resistive opposition. It is precisely this overlap that explains the broad shape of the phase peak and the fact that the Nyquist plot does not show two individual, perfectly separated semicircles.

For this circuit, the $\chi^2=3.35\cdot10^{-3}$ was obtained. The R(QR)(CR) circuit reproduces both the curvature observed in the Nyquist plot and the broad shape of the phase response in the Bode plot.

The CaZrZn sample after 60 days of immersion

At 60 days, the response of the CaZrZn sample changes significantly compared with that recorded after the first month of immersion. Whilst at 30 days the spectrum could be described by two capacitive-resistive contributions, without the introduction of a diffusion term, after 60 days the low-frequency behaviour indicates that species transport is beginning to play a more prominent role. This change necessitated a transition from the R(QR)(CR) circuit to the R(Q(RW))(CR) circuit.

The Nyquist plot (Fig. 19) remains open in the low-frequency range, without the tendency to close observed previously. At 0.01 Hz, Z' reaches ~17.54 kΩ·cm^2, and –Z'' at ~21.78 kΩ·cm^2, which corresponds to an impedance modulus of ~$2.80\cdot10^4$ Ω·cm^2. Compared with the values observed at 30 days, the low-frequency response is reduced. This suggests that, at this stage of immersion, the environment's access to the electrochemically active regions of the system is more pronounced.

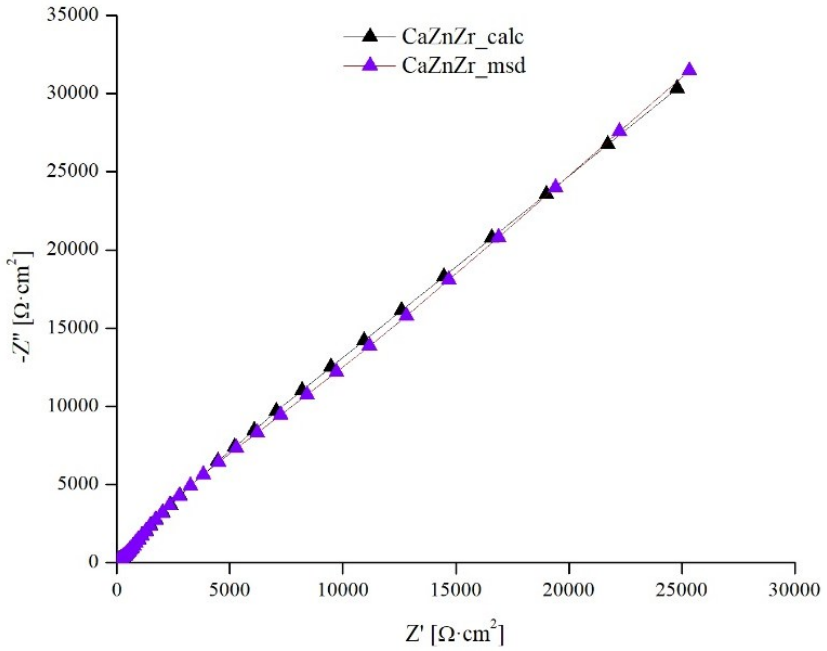

Fig. 19. The experimental Nyquist plot and the curve obtained by fitting for the CaZrZn layer after 60 days of immersion in DPBS

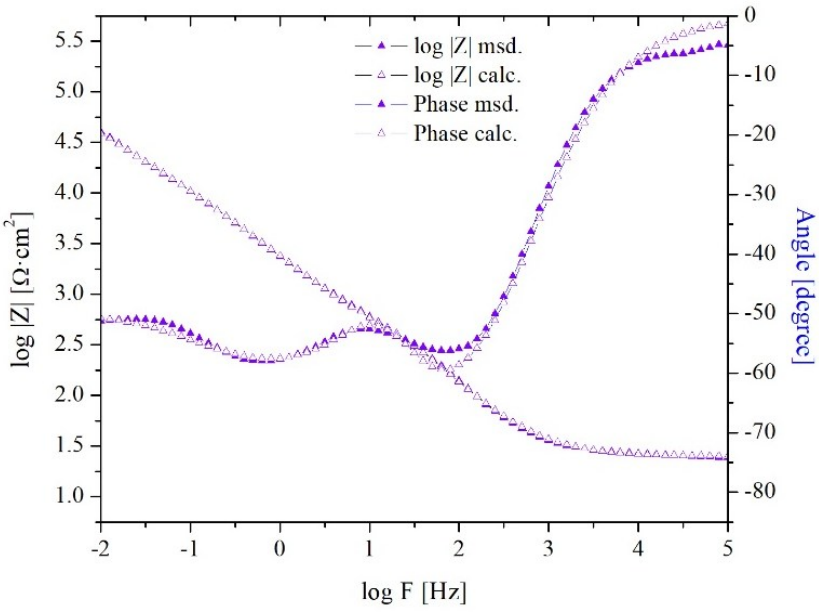

Fig. 20. Experimental Bode plot and the curve obtained by fitting for the CaZrZn layer after 60 days of immersion in DPBS

The phase angle, as seen in the Bode plot (Fig. 20), does not exhibit a single peak, but rather two broad regions of response. A peak of ~56º appears around 63 Hz, and a second, slightly higher peak of ~58º is observed around 0.63 Hz. The two regions partially overlap, which explains why no two distinct arcs are observed in the Nyquist plot. At 0.01 Hz, the phase angle remains at ~51º, whilst the impedance modulus continues to increase. This behaviour is consistent with the persistence of a transport contribution at long timescales and justifies the introduction of the Warburg term.

In the R(Q(RW))(CR) circuit, Fig. 10, R_s has a value of 24.92 $\Omega \cdot cm^2$, and its contribution to the total impedance is small. The dominant process is described by the Q(RW) branch. The constant-phase element has $Q = 1.11 \cdot 10^{-4}\ S \cdot s^n/cm^2$, and the exponent n = 0.72 is considerably lower than the value of n obtained after 30 days. The decrease in n indicates a more dispersed capacitive response and, consequently, an increase in the electrochemical non-uniformity of the system. After 60 days of contact with DPBS, the different regions of the layer no longer respond as uniformly, which may be associated with the gradual penetration of the medium through pores, crystalline boundaries or other discontinuities in the coating.

The resistance associated with this branch (R_1) is $\sim 2.60 \cdot 10^4\ \Omega \cdot cm^2$. This value is close to R_1, corresponding to the non-ideal branch at 30 days, which suggests that this resistive component does not disappear as the immersion period is extended. However, the nature of its response changes, such that at 60 days, the process is no longer adequately described by a QR combination alone; the Warburg contribution is also required.

The Warburg parameter has the value $W = 3.72 \cdot 10^{-5}\ S \cdot s^{0.5}/cm^2$ and explicitly incorporates the effect of species transport into the slow process. In this case, its presence may be linked to the movement of ions through the permeable zones of the layer and towards the interface with the substrate. This may suggest that mass transport becomes one of the components contributing to the system's overall response.

The CR fast branch is also maintained at 60 days. The capacitance associated with it is $C = 3.96 \cdot 10^{-5}\ F/cm^2$, and the resistance is only $R_2 = 167.9\ \Omega \cdot cm^2$. This resistance is much lower than that of the main process, so this branch does not control the overall electrochemical behaviour. The increase in capacitance compared with the value at 30 days cannot be interpreted

in isolation, as the circuit architecture has changed between the two time points. More relevant is the fact that the fast process remains detectable, whilst the slow response acquires an explicit transport component.

Consequently, the change observed between 30 and 60 days does not consist solely of a reduction in low-frequency impedance. The spectra also indicate an increase in electrochemical dispersion and the emergence of a more significant role for ionic transport. The layer continues to make a significant resistive contribution, but after 60 days, its behaviour can no longer be regarded as that of a predominantly capacitive barrier.

The R(Q(RW))(CR) circuit provides a good description of this evolution; the value $\chi^2=1.36\cdot10^{-3}$. In this case, the inclusion of the Warburg component is supported simultaneously by the Nyquist plot, by the maintenance of a high phase angle at low frequencies, and by the change in the shape of the spectrum compared with that observed after 30 days.

The CaZrZn sample after 90 days of immersion

After 90 days, the CaZrZn sample retains the same general response pattern observed at 60 days, which allows the spectrum to be described using the same circuit, R(Q(RW))(CR). Changes occur mainly in the amplitude and distribution of the electrochemical processes, without the need to introduce a new time constant. Low-frequency impedance remains high, but decreases slightly compared with the value recorded after 60 days.

In the Nyquist plot (Fig. 21), the curve remains open towards the low frequencies. At 0.01 Hz, Z' reaches ~17.78 kΩ·cm^2, and –Z'' at ~17.27 kΩ·cm^2, resulting in an impedance modulus of ~$2.48\cdot10^4$ Ω·cm^2. This value is slightly lower than the value of ~$2.80\cdot10^4$ Ω·cm^2 observed at 60 days; thus, between these two points in time, there is no sudden change in the overall impedance level, but rather a gradual evolution of the layer's response.

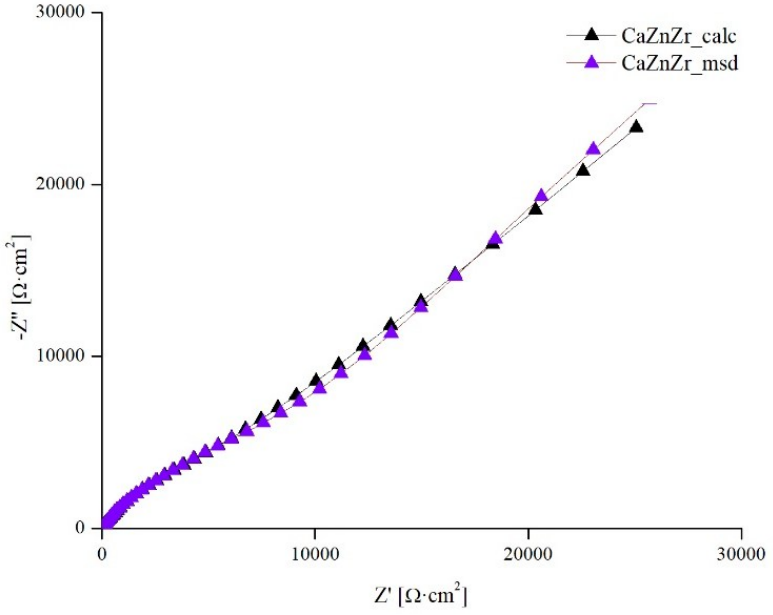

Fig. 21. The experimental Nyquist plot and the curve obtained by fitting for the CaZrZn layer after 90 days of immersion in DPBS

An interesting feature can be seen in the Bode plot (Fig. 22). The peak in the phase angle, of ~61.6°, is located around a frequency of 158 Hz, after which the phase decreases progressively towards lower frequencies. However, this decrease does not continue right down to the lower

limit of the frequency range. After values of ~39º around a frequency of 0.1 Hz, the angle increases again and reaches ~44.2º at 0.01 Hz. This rebound at very low frequencies is consistent with the persistence of a transport contribution and explains why the Warburg element remains necessary even after 90 days. At the same time, the impedance modulus increases from ~13.8 Ω·cm^2 at 100 kHz to ~24.8 kΩ·cm^2 at 0.01 Hz, without forming a plateau at the far end of the spectrum.

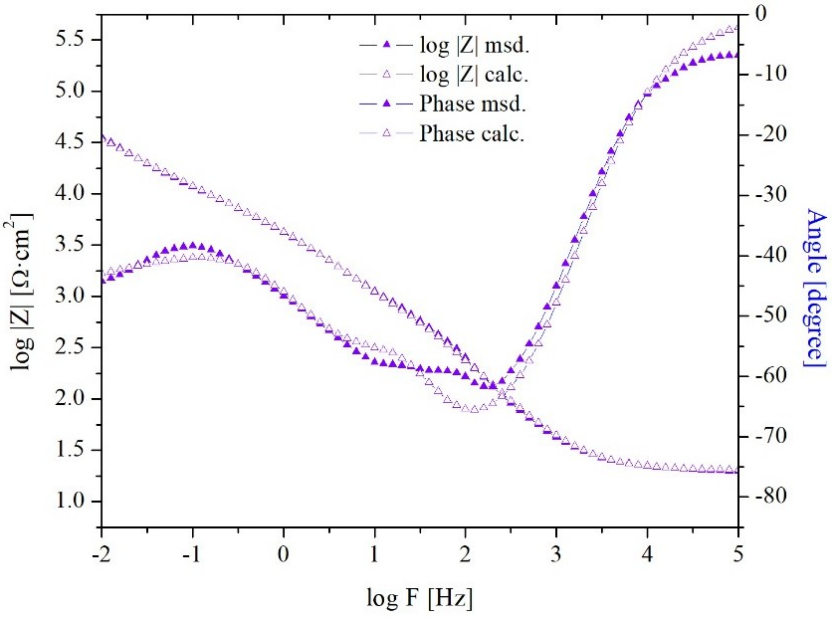

Fig. 22. Experimental Bode plot and the curve obtained by fitting for the CaZrZn layer after 90 days of immersion in DPBS

The R(Q(RW))(CR) circuit, Fig. 10, describes the response via a non-ideal capacitive process coupled with a transport contribution and via a second, faster, CR-type process. The resistivity of the solution is 20.16 Ω·cm^2, a small value compared with the other contributions, which indicates that the measured impedance is determined mainly by the behaviour of the layer and the interface.

For the main branch, the constant-phase element has $Q = 3.75 \cdot 10^{-5}$ S·s^n/cm^2 and n = 0.78. Compared with the value of n at 60 days, the increase in the exponent indicates a response somewhat closer to capacitive behaviour, although the surface clearly remains non-ideal. Thus, the electrochemical heterogeneity observed after 60 days does not disappear, but the distribution of time constants becomes less pronounced at the end of the immersion period.

The resistance associated with this contribution is $R_1=6.00 \cdot 10^3$ Ω·cm^2. The decrease, compared with that at 60 days, shows that the resistive opposition of the process described by the main branch decreases as exposure is prolonged. However, this trend is not accompanied by the disappearance of the capacitive behaviour or the transport contribution. Rather, after 90 days, the system reaches a state in which the electrolyte interacts more readily with the electrochemically active regions, whilst the layer continues to contribute to the overall response.

The Warburg element has $W = 1.16 \cdot 10^{-4}$ S·s$^{0.5}$/cm^2 and confirms that species transport remains relevant at long polarisation times. The change in the value of this parameter relative to the 60 day period should not be interpreted in isolation as a direct measure of an ‘increase’ or ‘decrease’ in diffusion; more importantly, the same type of contribution is required to describe both spectra. Thus, once it appears after 60 days, the transport-associated component persists up to 90 days.

The CR branch remains a secondary and transient contribution. The capacitance decreases to $2.41 \cdot 10^{-5}$ F/cm^2, whilst the associated resistance increases slightly to 203.4 $\Omega \cdot$cm^2. These values are much lower than those characteristic of the main process, which confirms that this branch does not control the low-frequency response. It can rather be regarded as the response of a surface region or of a process with a shorter time constant.

The results at 60 and 90 days show that the overall mechanism remains stable, but the relative contributions of its components change over time. The transport contribution is present at both time points, and the fast CR branch is maintained, whilst the resistance of the main process decreases and the capacitive character becomes somewhat more pronounced. This behaviour suggests a progressive evolution of the interface during prolonged contact with DPBS.

For 90 days, the circuit R(Q(RW))(CR) has $\chi^2=2.83 \cdot 10^{-3}$ and accurately reproduces both the Nyquist plot and the two characteristic regions observed in the Bode plot. Maintaining the same model between 60 and 90 days is also useful for a direct comparison of the parameters, showing that the observed changes are mainly quantitative, whilst the general nature of the electrochemical processes remains the same.

A comparison of the electrochemical behaviour of phosphate layers depending of immersion time

A comparison of the three variants shows that the differences between the phosphate layers obtained by chemical conversion are not limited to impedance levels, but also relate to the way in which each surface behaves during prolonged contact with DPBS. None of the samples exhibits a continuous and uniform decline in electrochemical response over the course of the 90 days. Instead, distinct stages are observed, in which the relative contributions of capacitive, resistive and ionic transport components change. This is significant because it shows that a comparison made after only 30 days would result in a different ranking to that obtained at the end of the test period.

After 30 days, ZnZrCa exhibits the highest low-frequency impedance modulus, followed by CaZrZn and ZrZnCa. From this perspective, ZnZrCa initially appears to be the most resistive of the three surfaces. However, the spectra show that the mechanisms underlying this response are different. ZnZrCa is described by two non-ideal time constants, (R(QR)(QR)), whilst for ZrZnCa it is necessary, even at this time scale, to introduce a Warburg component into the circuit (R(Q(RW))(CR)). CaZrZn occupies an intermediate position, its response being described by two capacitive-resistive contributions, (R(QR)(CR)), without diffusive transport being sufficiently pronounced as yet to require a Warburg element.

In ZnZrCa, the two time constants are characterised by very different CPE exponents, one close to 0.88 and the other approximately 0.64. This distinction suggests the coexistence of a region with a predominantly capacitive response and a much more heterogeneous one. For ZrZnCa, n has a value of approximately 0.83, and the low-frequency response is already influenced by species transport. CaZrZn exhibits an exponent close to 0.83 for the non-ideal component, but at the same time retains a second contribution that can be described by a capacitor. Thus, even though all samples have the same chemical basis, differences in composition lead, right from the first immersion stage, to interfaces with varying degrees of heterogeneity and permeability to the electrolyte.

The situation changes after 60 days. The low-frequency impedance decreases for all three variants compared with the initial values, and the differences between them become smaller. Consequently, the sample that exhibited the highest impedance after 30 days, ZnZrCa, reaches the lowest value of the three at this stage. This trend indicates that initial performance is not sufficient to predict behaviour following prolonged exposure.

For ZrZnCa, the 60-day period represents the most obvious mechanistic change. The circuit becomes (R(QR)(QR)W), requiring two distinct non-ideal capacitive contributions and a separate transport component. The similar values of the exponents of the two CPEs indicate that the two

processes exhibit similar degrees of non-ideality, even though their resistances differ significantly. At this stage, the ZrZnCa response appears to stem from a clearer separation between the different electrochemical regions of the layer, overlaid by ionic transport at low frequencies.

CaZrZn exhibits a different behaviour. The 30-day cycle is no longer sufficient, and at 60 days it becomes necessary (R(Q(RW))(CR)). The appearance of the Warburg element coincides with a reduction in the CPE exponent from approximately 0.83 to 0.72, which indicates a broader distribution of time constants and a more heterogeneous response. In the case of this sample, prolonging the immersion appears to favour the ingress of electrolyte through the permeable zones of the layer, such that species transport begins to contribute directly to the dominant process.

After 90 days, the differences between the samples become pronounced once again. ZrZnCa exhibits the highest low-frequency impedance, followed by ZnZrCa. For CaZrZn, the value continues to decrease slightly. At this stage, the order of the samples is almost the reverse of that observed initially: ZrZnCa, which after 30 days exhibited the lowest impedance of the three variants, becomes the most resistive following long-term exposure.

The most pronounced recovery is observed for ZrZnCa. At 90 days, the circuit reverts to (R(Q(RW))(CR)), a configuration also observed after 30 days, and the resistance of the main process increases considerably compared with the initial interval. The Warburg component remains present, indicating that the high impedance value should not be interpreted as evidence of a completely impermeable barrier. Species transport remains possible, but the electrochemical process at the interface encounters much greater resistance. This behaviour may reflect surface reorganisation during exposure, including changes to the layer and the formation of interfacial products in the phosphate medium. In the absence of structural characterisation following immersion, these mechanisms must, however, be considered possible explanations rather than directly attributed to a specific reaction product.

CaZrZn is the only variant for which the low-frequency impedance continues to decrease from the start to the end of the analysed period. The circuit (R(Q(RW))(CR)) remains stable for between 60 and 90 days, whilst the resistance of the main process continues to decrease. At the same time, the CPE exponent increases from approximately 0.72 to 0.78, indicating a slightly less dispersed response at the end of the test. Consequently, the decrease in the resistive contribution is not accompanied by a complete loss of the layer's capacitive nature. However, the persistence of the Warburg element shows that ionic transport through the system remains active even after 90 days.

The results highlight three different types of behaviour. ZnZrCa exhibits the greatest stability in terms of the electrochemical mechanism, as the same circuit with two time constants can describe all immersion intervals. The impedance varies considerably, but the general architecture of the response remains unchanged. CaZrZn exhibits the clearest trend towards a progressive reduction in the resistive contribution, accompanied by the emergence and persistence of diffusive transport after 60 days. ZrZnCa displays the most dynamic behaviour, with an intermediate stage in which the processes become more clearly separated, followed by a sharp increase in impedance at 90 days.

This comparison shows that immersion time and coating composition do not act independently. The composition determines how the coating responds to prolonged contact with DPBS, and this difference becomes more apparent as the exposure time increases. If the analysis had been limited to 30 days, ZnZrCa might have been considered the variant with the most favourable electrochemical response. After 90 days, however, ZrZnCa exhibits the highest low-frequency impedance and the strongest resistive contribution among the variants analysed. In contrast, CaZrZn exhibits a progressive reduction in electrochemical resistance.

Consequently, ZrZnCa appears to be the most promising variant for long-term exposure in DPBS, even though its response at intermediate time intervals is more complex. The results

confirm that evaluating phosphate coatings only immediately after preparation or after a single immersion period may lead to incomplete conclusions. Successive monitoring via EIS provides a more accurate picture of the actual evolution of the interface and allows a distinction to be made between a progressive loss of protective properties, a simple temporary change in response, and a reorganisation of the system during prolonged exposure.

Conclusions

The electrochemical behaviour of the three layers was monitored in DPBS over an extended period of immersion. The results show that their behaviour cannot be described by a simple, continuous degradation process, but rather by successive changes in the capacitive response, the resistive contributions and the ionic transport through the layer and towards the interface. Thus, it was observed that:

- The ZnZrCa sample maintained the same general pattern of electrochemical response throughout the entire period analysed. The persistence of the two-time-constant circuit suggests that the processes associated with the layer and the interfacial region remain distinct, even though their relative proportions change over time.
- For ZrZnCa, the influence of the immersion time was more pronounced. The change in the equivalent circuit at the intermediate frequency range shows a clearer separation of the electrochemical processes and a greater contribution from species transport at low frequencies. At the end of the exposure period, however, the response indicates that a significant electrochemical barrier is maintained, making this variant the most promising of those analysed for prolonged exposure in DPBS.
- The CaZrZn sample initially exhibited a response dominated by two capacitive-resistive contributions, whilst after prolonged immersion it became necessary to include a Warburg component. This change suggests that ionic transport through the permeable regions of the layer plays an increasingly important role over time, without the system's capacitive response disappearing.

Overall, the three layers exhibit different electrochemical behaviours, which confirms the influence of composition on long-term stability. ZnZrCa is characterised by a relatively stable mechanism, CaZrZn by an increasingly noticeable contribution from transport processes, and ZrZnCa by a more complex reorganisation of the interface, followed by favourable electrochemical behaviour at the end of the test period. The results thus support the use of long-term EIS monitoring to differentiate the performance of phosphate coatings, as evaluation at a single immersion interval may lead to incomplete conclusions.

Acknowledgment

This work was supported by a grant of the Ministry of Research, Innovation and Digitalization, CNCS-UEFISCDI, project number PN-IV-P2-2.1-TE-2023-1086.

The authors acknowledge the use of AI-assisted tools for language refinement, text organization, and readability improvement during manuscript preparation. The scientific content, interpretation, conclusions, and final manuscript were reviewed and validated by the authors, who take full responsibility for the work.

Funding body

This work was supported by a grant of the Ministry of Research, Innovation and Digitalization, CNCS-UEFISCDI, project number PN-IV-P2-2.1-TE-2023-1086.

Author Contributions

Diana Petronela Burduhos Nergis: Conceptualization, Investigation, Methodology, Visualization, Funding Acquisition, Writing – original draft, Project administration; **Andrei Victor Sandu**: Conceptualization, Methodology, Writing – review & editing, Investigation; **Luminita-Gabriela Mutila:** Investigation, Methodology, Visualization; **Costica Bejinariu:** Conceptualization, Methodology, Supervision, Validation, Writing – review & editing; **Petrica Vizureanu**: Conceptualization, Data curation, Investigation, Methodology, Visualization, Writing – review & editing.

References

[1] S. Gudić, L. Vrsalović, D. Kvrgić, and A. Nagode, "Electrochemical Behaviour of Ti and Ti-6Al-4V Alloy in Phosphate Buffered Saline Solution," *Materials 2021, Vol. 14,* vol. 14, no. 24, Dec. 2021, doi: 10.3390/MA14247495.

[2] D. P. Burduhos-Nergis, D. D. Burduhos-Nergis, S. M. Baltatu, and P. Vizureanu, "Advanced Coatings for the Corrosion Protection of Metals," vol. 115, Jan. 2022, doi: 10.21741/9781644901670.

[3] B. Liu, X. ming Shi, G. yong Xiao, and Y. peng Lu, "In-situ preparation of scholzite conversion coatings on titanium and Ti-6Al-4V for biomedical applications," *Colloids Surf. B Biointerfaces*, vol. 153, pp. 291–299, May 2017, doi: 10.1016/J.COLSURFB.2017.03.007.

[4] B. Liu, G. Xiao, and Y. Lu, "Effect of pH on the Phase Composition and Corrosion Characteristics of Calcium Zinc Phosphate Conversion Coatings on Titanium," *J. Electrochem. Soc.*, vol. 163, no. 8, pp. C477–C485, Jun. 2016, doi: 10.1149/2.0921608JES/XML.

[5] B. Liu, G. yong Xiao, C. zhong Chen, Y. peng Lu, and X. wen Geng, "Hopeite and scholzite coatings formation on titanium via wet-chemical conversion with controlled temperature," *Surf. Coat. Technol.*, vol. 384, p. 125330, Feb. 2020, doi: 10.1016/J.SURFCOAT.2019.125330.

[6] Y. Y. Guo *et al.*, "Antibacterial activity and increased osteoblast cell functions of zinc calcium phosphate chemical conversion on titanium," *Surf. Coat. Technol.*, vol. 294, pp. 131–138, May 2016, doi: 10.1016/J.SURFCOAT.2016.03.085.

[7] D. P. Burduhos-Nergis, N. Cimpoesu, E. L. Epure, B. Istrate, D. D. Burduhos-Nergis, and C. Bejinariu, "Ca–Zn Phosphate Conversion Coatings Deposited on Ti6Al4V for Medical Applications," *Coatings 2023, Vol. 13, Page 1029*, vol. 13, no. 6, p. 1029, Jun. 2023, doi: 10.3390/COATINGS13061029.

[8] K. Zuo *et al.*, "Zinc-Doping Induces Evolution of Biocompatible Strontium–Calcium-Phosphate Conversion Coating on Titanium to Improve Antibacterial Property," *ACS Appl. Mater. Interfaces*, vol. 14, no. 6, pp. 7690–7705, Feb. 2022, doi: 10.1021/ACSAMI.1C23631.

[9] D. W. Zhao *et al.*, "Strontium-zinc phosphate chemical conversion coating improves the osseointegration of titanium implants by regulating macrophage polarization," *Chemical Engineering Journal*, vol. 408, p. 127362, Mar. 2021, doi: 10.1016/J.CEJ.2020.127362.

[10] D. P. Burduhos-Nergis *et al.*, "Micromorphology and properties of novel phosphate conversion coatings based on zinc-magnesium and zinc-zirconium deposited on Ti6Al4V,"

Surfaces and Interfaces, vol. 76, p. 107884, Nov. 2025, doi: 10.1016/J.SURFIN.2025.107884.

[11] C. Bejinariu, D.-P. Burduhos-Nergis, and N. Cimpoesu, "Immersion Behavior of Carbon Steel, Phosphate Carbon Steel and Phosphate and Painted Carbon Steel in Saltwater," *Materials*, vol. 14, no. 1, p. 188, Jan. 2021, doi: 10.3390/ma14010188.

[12] Y.-B. ; Li *et al.*, "Effect of Reaction Temperature on the Microstructure and Properties of Magnesium Phosphate Chemical Conversion Coatings on Titanium," *Molecules 2023, Vol. 28, Page 4495*, vol. 28, no. 11, p. 4495, Jun. 2023, doi: 10.3390/MOLECULES28114495.

Received: June 13, 2026
Accepted: August 22, 2026